MCH5 column, equilibrated with buffer A. Unreacted iodide passed through the column. After switching to buffer B, [^{123}I-Tyr^{A19}]insulin, unlabeled insulin, and [^{123}I-Tyr^{A14}]insulin were successively eluted. Elution buffers contained tris (0.5 mole/liter), phosphoric acid (0.25 mole/liter), EDTA (5 mmole/liter), and either 20 percent (buffer A) or 38 percent (buffer B) absolute ethanol; the *p*H was adjusted to 7 with tris.
7. The theoretical values of the specific activity are 41 mCi/μg for ^{123}I-labeled monoiodoinsulin and 0.37 mCi/μg for ^{125}I-labeled monoiodoinsulin.
8. S. Terris and D. F. Steiner, *J. Clin. Invest.* **57**, 885 (1976).
9. J. C. Sodoyez, F. Sodoyez-Goffaux, Y. M. Moris, *Am. J. Physiol.* **239**, E3 (1980).
10. Liver extraction of [^{123}I]insulin was inhibited by prior injection of antiserum to the insulin receptor (J. C. Sodoyez, F. Sodoyez-Goffaux, S. Treves, E. R. Kahn, in preparation).
11. M. J. Chamberlain and L. Stimmler, *J. Clin. Invest.* **46**, 911 (1967).
12. W. Meier-Ruge and F. Fridrich, *Histochemie* **19**, 147 (1969).
13. J. J. M. Bergeron, R. Rachubinski, N. Searle, D. Borts, R. Sikstrom, B. I. Posner, *J. Histochem. Cytochem.* **28**, 824 (1980); J. J. M. Bergeron *et al.*, *Endocrinology* **107**, 1069 (1980); F. Sodoyez-Goffaux, J. C. Sodoyez, C. J. De Vos, *Diabetes* **31**, 60 (1982); F. Sodoyez-Goffaux, unpublished observations.
14. I. B. Syed and F. Hosain, in *Handbook Series in Clinical Laboratory Science*, section A, *Nuclear Medicine*, D. Seligson, Ed. (CRC Press, Boca Raton, Fla., 1982), vol. 2, p. 169; J. A. Jungerman and M. C. Lagunas-Solar, *J. Radioanal. Chem.* **65**, 31 (1981).
15. This work was supported by grants from the National Fund for Scientific Research, Brussels, Belgium. We thank Ch. Fallais for the generous gift of Na^{123}I, C. R. Kahn for editorial help, and S. Segal and M. Fodor for secretarial assistance.

2 November 1982

Actin Filament Stress Fibers in Vascular Endothelial Cells in vivo

Abstract. *Fluorescence microscopy with 7-nitrobenz-2-oxa-3-diazole phallacidin was used to survey vertebrate tissues for actin filament bundles comparable to the stress fibers of cultured cells. Such bundles were found only in vascular endothelial cells. Like the stress fibers of cultured cells, these actin filament bundles were stained in a punctate pattern by fluorescent antibodies to both alpha-actinin and myosin. The stress fibers were oriented parallel to the direction of blood flow and were prominent in endothelial cells from regions exposed to high-velocity flow, such as the left ventricle, aortic valve, and aorta. Actin bundles may help the endothelial cell to withstand hemodynamic stress.*

Stress fibers (*1*), bundles of actin filaments containing myosin and α-actinin (*2*), are found in many cultured cells, but little is known about the existence of comparable actin filament bundles in living organisms. Actin bundles were recently detected in fish scales (*3*) and conifer roots (*4*) by fluorescence methods. Similar bundles have not been detected in higher vertebrates by immunofluorescence, but have been observed in the vascular endothelium by electron microscopy (*5*). The filaments in these bundles are the right size (6 to 7 nm) to be actin, and some bundles even have electron-dense bodies like stress fibers. On the other hand, the failure to detect these bundles with fluorescent antibodies to actin (*6*) casts doubt on their similarity to stress fibers. Furthermore, it has not been established whether the endothelial cell filament bundles are similar to stress fibers with respect to their distribution of myosin or α-actinin.

In this study we searched numerous vertebrate tissues for cells with actin filament bundles comparable to the stress fibers of cultured cells. We employed the fluorescence microscope with the reagent 7-nitrobenz-2-oxa-3-diazole (NBD) phallacidin as a probe (*7*). Phallacidin is an acidic derivative of phalloidine, one of the phallotoxins isolated from the mushroom *Amanita phalloides*. This toxin binds to actin filaments with high affinity (*8*). We also used fluorescent antibodies to myosin (*9*) and α-actinin (*10*) to identify the contractile proteins.

In our search we examined cryostat sections of rat cortex, cerebellum, spinal cord, sciatic nerve, epidermis, liver, bone marrow, and bovine aortic valve; smears of human peripheral blood and rat bone marrow; whole mounts of rat mesentery and brain leptomeninges; and monolayers of rat lung pleura, liver mesothelium, arachnoid mater, and bovine and chicken endothelial cells. NBD phallacidin either stained the ectoplasm of these cells more densely than the inner portion or stained the cytoplasm uniformly. Cells with the former staining pattern included motor neurons, hepatocytes, and squamous cells of the epidermis, mesothelium, pleura, and arachnoid mater. Diffuse fluorescence was found in the cell bodies of cortical and cerebellar neurons and in lymphocytes. Megakaryocytes in both smears and sections contained a lacy network not reminiscent of stress fibers.

The only actin filament bundles similar to stress fibers were found in a subset of the vascular endothelial cells of cows, chickens, dogs, rats, and a cat (Fig. 1). Although these cells vary in their morphology throughout the vasculature, each showed intense NBD phallacidin staining around its periphery (Fig. 1). In parts of the vasculature subjected to blood flow of high velocity and turbulence, the endothelial cells also contained fibers that were stained by NBD phallacidin and antibodies to actin, myosin, and α-actinin. In the cows these actin filament bundles were about 0.2 μm wide and up to 10 μm long and were always oriented parallel to the direction of blood flow. Endothelial cells with actin bundles were found in the chambers of the heart, aortic valve, and aorta (Fig. 1), but the number and size of the bundles varied, as did the shape of the cells. Actin bundles were particularly prominent in the ventricles, left atrium, and aorta. In the aorta the cells and fibers were oriented in the direction of blood flow. Endothelial cells from the vena cava were polygonal and had very few or no actin bundles (Fig. 1G).

Endothelial cell morphology varied in the different regions of the aortic valve. At the base (on either side) the cells were spindle-shaped and had very prominent actin bundles oriented parallel to the blood flow (Fig. 1, H to J). In the middle of the valve the endothelial cells were larger and oval, but the stress fibers were still oriented in the direction of flow. The cells at the valve tip were rounded and had a large nucleus and no actin fibers.

The chicken endothelial cells were similar to those of the cows in overall morphology and staining with NBD phallacidin. We stained endothelial cells of chicken aorta simultaneously with NBD phallacidin and rhodamine-labeled antibodies to chicken gizzard α-actinin (Fig. 1L) or platelet myosin (Fig. 1N). The NBD phallacidin staining of stress fibers was continuous whereas the staining with the antibodies was punctate.

The specificity of the fluorescent reagents for endothelial cells was established by showing that a 50-fold molar excess of unlabeled phalloidine competitively inhibited NBD phallacidin staining (Fig. 1O). Controls for the antibodies have been described by Herman *et al.* (*9*).

The inferior vena cava of dogs, rabbits, rats, and a cat contained almost no stress fibers. In all these species the aortic endothelial cells had actin filament bundles similar to those in the cow aorta, but the bundles were less prominent in the chambers of the heart than in cows. In most cases there were more actin filament bundles in the proximal than distal portions of the aorta, but this situation was reversed in the rat. It remains to

be established whether these quantitative differences are due to species variations in the adaptation of endothelial cells to hemodynamic forces or to the fact that the forces in the same parts of the vasculature differ among the species.

We have established that endothelial cells have actin filament bundles containing punctate regions with high concentrations of α-actinin and myosin. In terms of morphology and protein composition they closely resemble the stress fibers of cultured cells. Similar stress fibers were not detected in a large sample of cells from other vertebrate tissues. Unlike the stress fibers of cultured cells, some of the endothelial cell stress fibers were wavy or kinked. We expect, however, that they were straight when under tension in situ.

The similarities in morphology and protein composition suggest that the actin bundles of endothelial cells and the stress fibers of cultured cells have the same functions. It has been demonstrated that in permeabilized model systems of cultured cells, stress fibers can contract (*11*), and it seems likely that the stress fibers exert tension on the substrate at the focal contacts where they insert into the plasma membrane (*12*). In this way, they help to anchor the cell to the substrate (*1*). We believe that the endothelial cell stress fibers have a similar structural role in distributing forces applied to the free surface and cytoplasm to attachment sites on the basement membrane. The orientation of the stress fibers parallel to the direction of blood flow and the direct correlation between stress fiber number and blood velocity support this speculation. Our interpretation is backed by a preliminary report showing that the stress fibers of cultured endothelial cells realign in the direction of an applied flow (*13*).

The shearing force of blood may be a determinant of endothelial cell stress fiber elaboration and orientation, but the relation between stress fibers and the shearing force appears complex. The endothelium also experiences tension from blood pressure exerted around the wall of the vessel, orthogonal to the shearing force. Considering the longitudinal orientation of the individual cell, the shearing force may be predominant. However, another consideration is the effect of curvature. Dunn and Heath (*14*) demonstrated that cells seeded onto capillary

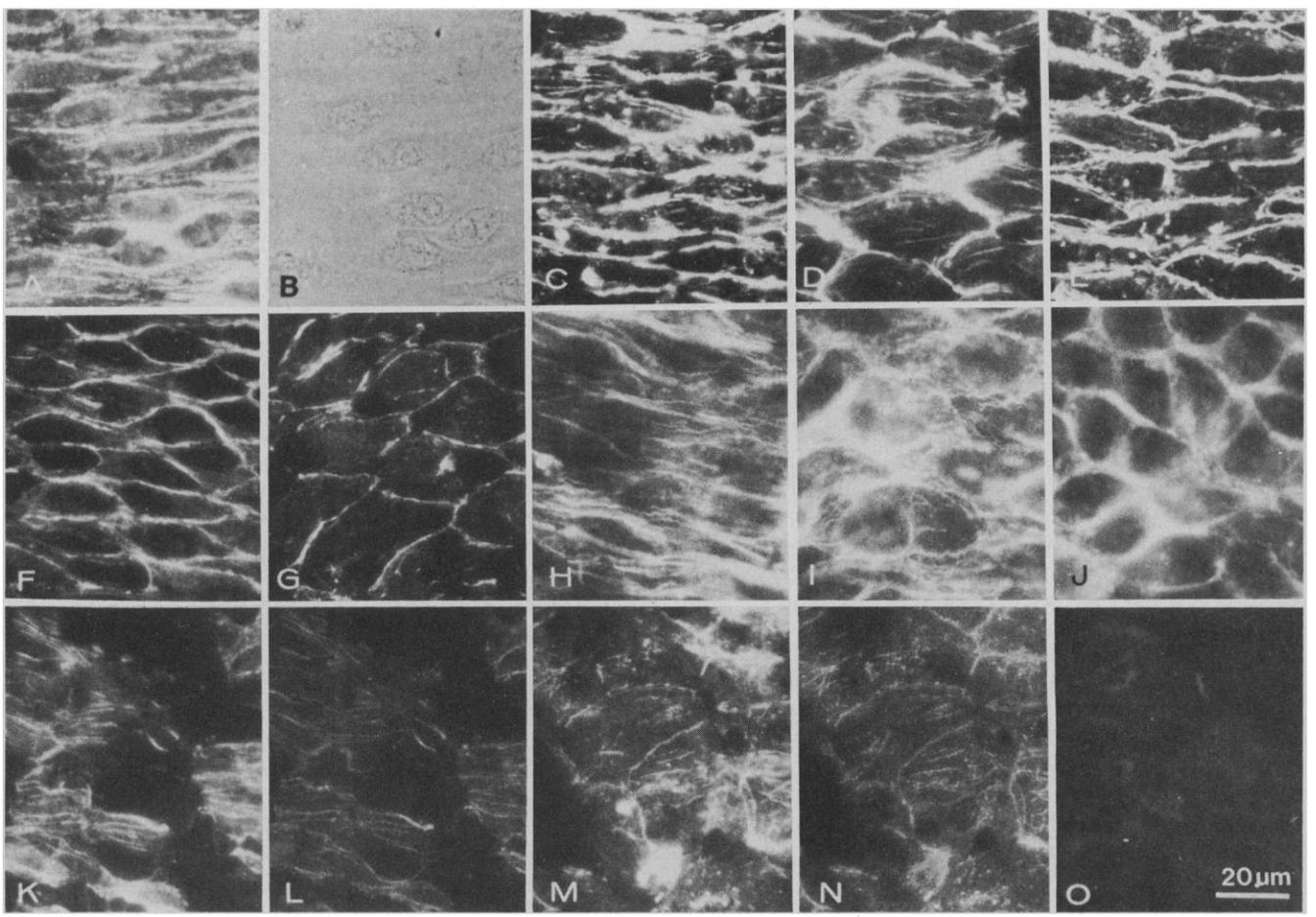

Fig. 1. Fluorescence and phase-contrast micrographs of endothelial cells stained for actin with NBD phallacidin (A to K; M) or stained for α-actinin (L) or myosin (N) with fluorescent antibodies. Sheets of endothelial cells were removed from bovine aorta (A and B), bovine ventricle (C), bovine left atrium (D), bovine right ventricle (E), bovine right atrium (F), bovine superior vena cava (G), the base of the bovine aortic valve (H), the midportion of the same valve (I), the tip of the same valve (J), chicken aorta (K and L), and bovine left ventricle (M). The control preparation consisted of bovine aortic endothelial cells stained with NBD phallacidine and a 50-fold molar excess of unlabeled phalloidine (O). Endothelial cell monolayers were prepared by a modification of the method of Warren (*15*). Tissues were dissected from freshly slaughtered cows or chickens and placed endothelium-side-down on a slide, with care being taken not to distort the tissue excessively. The assembly was immersed in *N*-methylbutane cooled to −56°C with dry ice and then transferred to a cryostat at −20°C, where the bulk of the tissue was grasped with forceps and peeled off. Alternatively, a surgical blade was inserted between tissue and slide and twisted to remove the block of tissue. The tissue reproducibly cleaves along the basal lamina, leaving a monolayer of epithelial cells adhering to the slide. The slide was then dried at room temperature for 1 hour under a fan. The cells were made permeable by immersion in acetone at 20°C for 30 seconds, air-dried, rinsed in phosphate-buffered saline, dried once more, and stained with NBD phallacidin (0.2 μg/ml) (*7*) in phosphate-buffered saline for 20 minutes at room temperature. After a 5-minute wash in saline, the slides were dried and mounted in 90 percent glycerol and 10 percent saline.

tubes orient themselves longitudinally rather than circumferentially. The effect of curvature may be important, especially in small vessels, where the effect on individual cells is the greatest.

Adaptive alterations in endothelial cell stress fibers seem likely in disease processes such as hypertension and atherosclerosis. An increase in the concentration of endothelial actin in hypertension has been suggested by staining with fluorescent antibodies (*6*), so a reevaluation with our techniques might be informative.

ALBERT J. WONG
THOMAS D. POLLARD
Department of Cell Biology and Anatomy, Johns Hopkins School of Medicine, Baltimore, Maryland 21205
IRA M. HERMAN*
Department of Anatomy and Cellular Biology, Tufts University School of Medicine, Boston, Massachusetts 02111

References

1. W. H. Lewis and M. K. Lewis, in *General Cytology*, E. V. Cowdry, Ed. (Univ. of Chicago Press, Chicago, 1924), pp. 385–447; E. Lazarides and K. Weber, *Proc. Natl. Acad. Sci. U.S.A.* **71**, 2268 (1974); E. Lazarides and K. Burridge, *Cell* **6**, 289 (1975); I. M. Herman and T. D. Pollard, *J. Cell Biol.* **80**, 509 (1979); T. E. Kreis and W. Birchmeir, *Cell* **22**, 555 (1980).
2. K. Weber and U. Groschel-Stewart, *Proc. Natl. Acad. Sci. U.S.A.* **71**, 4561 (1974); E. Lazarides, *J. Cell Biol.* **68**, 202 (1976).
3. H. R. Beyers and K. Fujiwara, *J. Cell Biol.* **93**, 804 (1982).
4. T. C. Pesacreta, W. W. Carley, W. W. Webb, M. V. Parthasarathy, *Proc. Natl. Acad. Sci. U.S.A.* **79**, 2898 (1982).
5. F. Hammersen, *Adv. Microcirc.* **9**, 95 (1980).
6. G. Gabbiani, M. C. Badonnel, G. Rona, *Lab. Invest.* **32**, 277 (1975); G. Gabbiani, G. Elemer, C. Guelpa, M. B. Vallotton, M. C. Badonnel, J. Huttner, *Am. J. Pathol.* **96**, 399 (1979).
7. L. S. Barak, R. R. Yocum, E. A. Nothnagel, W. W. Webb, *Proc. Natl. Acad. Sci. U.S.A.* **77**, 980 (1980); L. S. Barak and R. R. Yocum, *Anal. Biochem.* **110**, 31 (1981).
8. T. Wieland, H. Faulstein, *CRC Crit. Rev. Biochem.* **5**, 185 (1978); J. D. Estes, L. A. Selden, L. C. Gerhsam, *Biochemistry* **20**, 708 (1981).
9. I. M. Herman, N. Crisona, T. D. Pollard, *J. Cell Biol.* **90**, 84 (1981).
10. K. Fujiwara, M. Porter, T. D. Pollard, *ibid.* **79**, 268 (1978).
11. G. Isenberg, P. C. Rathke, N. Hulsmann, W. Franke, K. E. Wolfarth-Botterman, *Cell Tissue Res.* **166**, 427 (1976); T. E. Kreis and W. Birchmeir, in (*1*).
12. A. K. Harris, D. Stopak, P. Wild, *Nature (London)* **290**, 249 (1981).
13. G. E. White *et al.*, *Fed. Proc. Fed. Am. Soc. Exp. Biol.* **41**, 321 (1982).
14. G. A. Dunn and J. P. Heath, *Exp. Cell Res.* **101**, 1 (1976).
15. B. A. Warren, *J. R. Microsc. Soc.* **84**, 407 (1965).
16. Supported by NIH grant GM26338-03 and a Muscular Dystrophy Association of America postdoctoral fellowship to I.M.H. We thank J. Griffin for providing facilities and L. Barak for providing NBD phallacidin.
* To whom correspondence should be addressed.
18 May 1982; revised 12 October 1982

Intracellular Calcium Measurements with Arsenazo III During Cyclic AMP Injections into Molluscan Neurons

Abstract. *Injections of cyclic adenosine monophosphate into molluscan neurons often produce a transient membrane depolarization. By using the calcium indicator dye arsenazo III, it was found that cyclic nucleotide injections into neurons of* Archidoris montereyensis *resulted in elevation of internal calcium concentrations. However, this was demonstrated to be a secondary consequence of an induced increase in membrane sodium permeability, and not due to any direct effect of cyclic adenosine monophosphate on cellular calcium influx or internal calcium regulating processes.*

Many different types of cells utilize intracellular second messengers, such as cyclic adenosine monophosphate (AMP), cyclic guanosine monophosphate (GMP), and Ca^{2+}, to transduce membrane signals into a wide range of cellular responses (*1*). Evidence has been accumulating that the concentration of these messengers is regulated not only by extracellular effectors—that is, first messengers such as hormones and neurotransmitters—but also through feedback relations with each other (*2, 3*). For example, there is considerable indirect evidence that elevation of the internal cyclic AMP concentration leads to an increase in the intracellular calcium concentration, $[Ca^{2+}]$, in cells exhibiting stimulus-secretion coupling, such as nerve terminals and endocrine cells (*3*). However, there are no direct measurements of such increases, nor clear indications of the mechanism or mechanisms that bring them about.

Intracellular injections of cyclic AMP or its derivatives into mammalian (*4*) and molluscan neurons (*5, 6*) have been reported to produce membrane depolarizations or increases in net inward current. In one reported instance this effect was shown to be the direct result of an induced calcium influx (*6*). However, in most instances the mechanism of action of cyclic AMP has not yet been deduced. We report here measurements on a set of reidentifiable molluscan neurons which show that increased intracellular levels of cyclic AMP do indeed lead to increased cellular $[Ca^{2+}]$, but that the coupling mechanism is indirect.

Giant neurons (~ 300 to 500 μm in diameter) within isolated ganglia from the circumoesophageal ring ganglia of *Archidoris montereyensis* were maintained in vitro at 12°C in a physiological saline of the following composition: 490 m*M* NaCl, 8 m*M* KCl, 10 m*M* $CaCl_2$, 20 m*M* $MgCl_2$, 30 m*M* $MgSO_4$, 10 m*M* MOPS, 5 m*M* glucose, and *p*H adjusted to 7.6. Recording electrodes were filled with 3*M* KCl and had resistances of 1 to 2 megohms. Standard two-electrode voltage clamping techniques were employed. Iontophoresis electrodes were filled with 0.1*M* HCl, 0.2*M* $CaCl_2$, or 0.2*M* cyclic AMP (grade I, Sigma). Pressure injection electrodes were filled with a buffered cyclic AMP solution (0.2*M*) at *p*H 7.4. We constructed *p*H microelectrodes according to procedures described by Thomas (*7*). The *p*H microelectrodes had tip diameters of 1 to 2 μm and response times—that is, 90 percent completion following a step change in *p*H—of approximately 1.5 minutes. We used *p*H electrodes with slopes of 54 to 58 mV per unit of *p*H change.

The indicator dye arsenazo III (grade I, Sigma) was used to examine changes in intracellular free Ca^{2+}. This dye has been used extensively for monitoring changes in cellular $[Ca^{2+}]$ (*8–14*). Neurons were iontophoretically injected with dye (10 mg/ml) under voltage clamp, using pulses of 200 to 400 nA for 0.8 second repeated at 1 Hz. Injections were quantified as described elsewhere (*12–14*). The dye is nontoxic when loaded into cells at concentrations up to 1 m*M*, and at this concentration it can detect submicromolar changes in cellular $[Ca^{2+}]$ (*15*). Changes in internal Ca^{2+} were detected by monitoring the absorbance of the dye at the differential wavelength pair 660 − 700 nm with a rotating wheel spectrophotometer (*16*).

Figure 1A shows the recording arrangement, and Fig. 1, B and C, shows records of experiments during which separate injections of Ca^{2+} and H^+ were made into a neuron containing 0.3 m*M* arsenazo III. Dye absorbance was simultaneously monitored at two wavelength pairs, 660 − 700 nm and 610 − 700 nm. These dual-wavelength measurements were used in order to reduce light scattering or dilution artifacts by subtracting a relatively ion-insensitive wavelength (700 nm) from the recording. Calcium ion injection resulted in a greater increase in absorbance at 660 − 700 nm than at 610 − 700 nm, a result at odds with in vitro dye measurements (*9*) but consistent with in situ results (*10, 12*). The subsequent recoveries of the absorbance signals were analyzed and are thought to result from cellular calcium buffering systems, cellular extrusion of calcium,